Supplementary Information (SI) for Journal of Materials Chemistry C.

Anti-Naphthalene Bisbenzimidazole Columnar Mesogens as Interfacial Modifiers in Perovskite Solar Cells

Ankita Sharma[a], Paresh Kumar Behera[b], Kajal Yadav[a], Tarun[a], Pankaj Yadav[c], Ammathnadu Sudhakar Achalkumar [b,d*], Upendra Kumar Pandey[a*]

[a,] *Organic & Flexible Electronics Laboratory, Department of Electrical Engineering, School of Engineering, Shiv Nadar Institution of Eminence, G.B. Nagar, Uttar Pradesh- 201314, India.*
[b]*Department of Chemistry, Indian Institute of Technology Guwahati, Guwahati, Assam-781039, India.*
[c]*Department of Solar Energy, School of Technology, Pandit Deendayal Energy University, Gandhinagar, Gujarat-382 007, India*

[d]*Centre for Sustainable Polymers, Indian Institute of Technology Guwahati, Guwahati, Assam-781039, India*

Email: upendra.pandey@snu.edu.in , achalkumar@iitg.ac.in

Contents

1. Surface Profilometry: 3
2. X-ray Diffraction (XRD) Analysis: 4
3. Field Emission Scanning Electron Microscopy (FESEM): 6
4. Ultraviolet-Visible Spectroscopy: 7
5. Time-resolved photoluminescence (TRPL) Spectra: 9
6. Current Density-Voltage (*J-V*) Characteristics 10
7. Histogram Analysis 12
8. Hysteresis Index Evaluation. 13
9. Electrochemical Impedance Spectroscopy (EIS): 14
10. Fabrication of SCLC Devices for Mobility and Trap Density Analysis 14
11. References 18

1. Surface Profilometry:

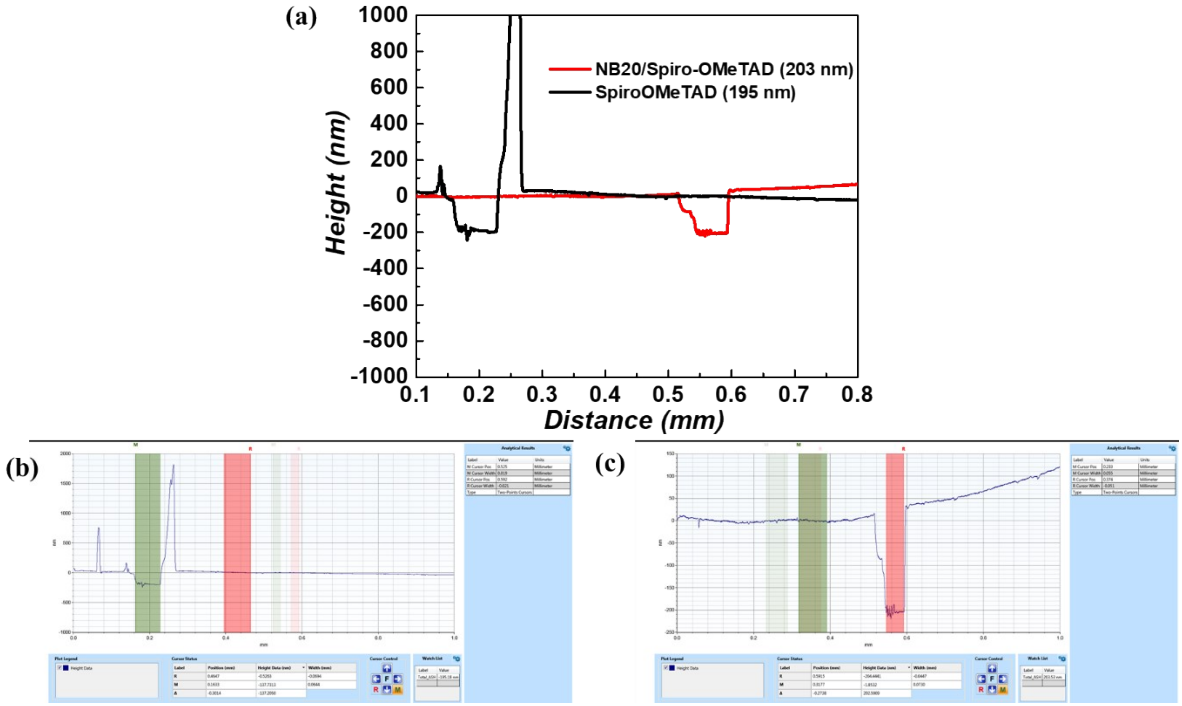

Figure S1. (a) Surface profilometry of Spiro-OMeTAD and NB20/Spiro-OMeTAD, (b) and (c) corresponding raw data extracted from the profilometer measurements.

2. X-ray Diffraction (XRD) Analysis:

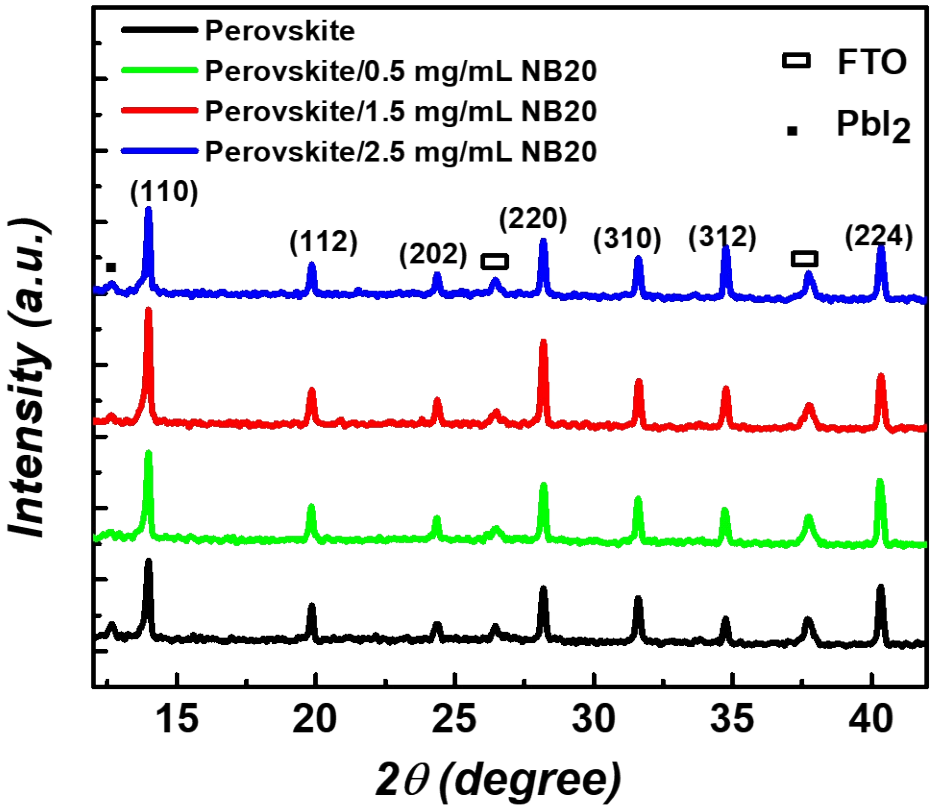

Figure S2. Structural properties characterization via XRD of perovskite films incorporating varying concentrations of NB20.

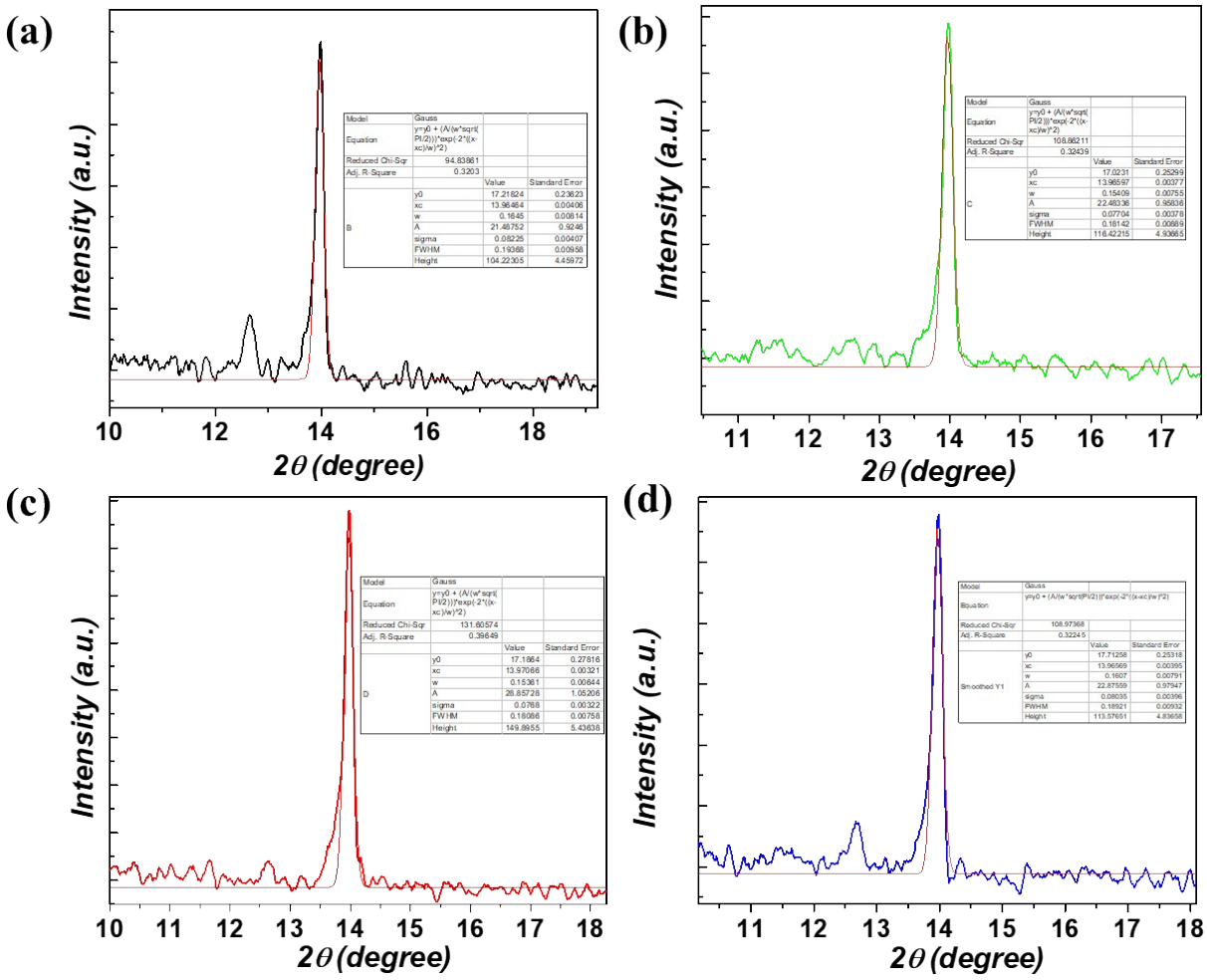

Figure S3. Fitted XRD diffraction peak for perovskite films with NB20 at different concentrations. The fitted parameters (FWHM, and peak height) are shown in the inset tables.

3. Field Emission Scanning Electron Microscopy (FESEM):

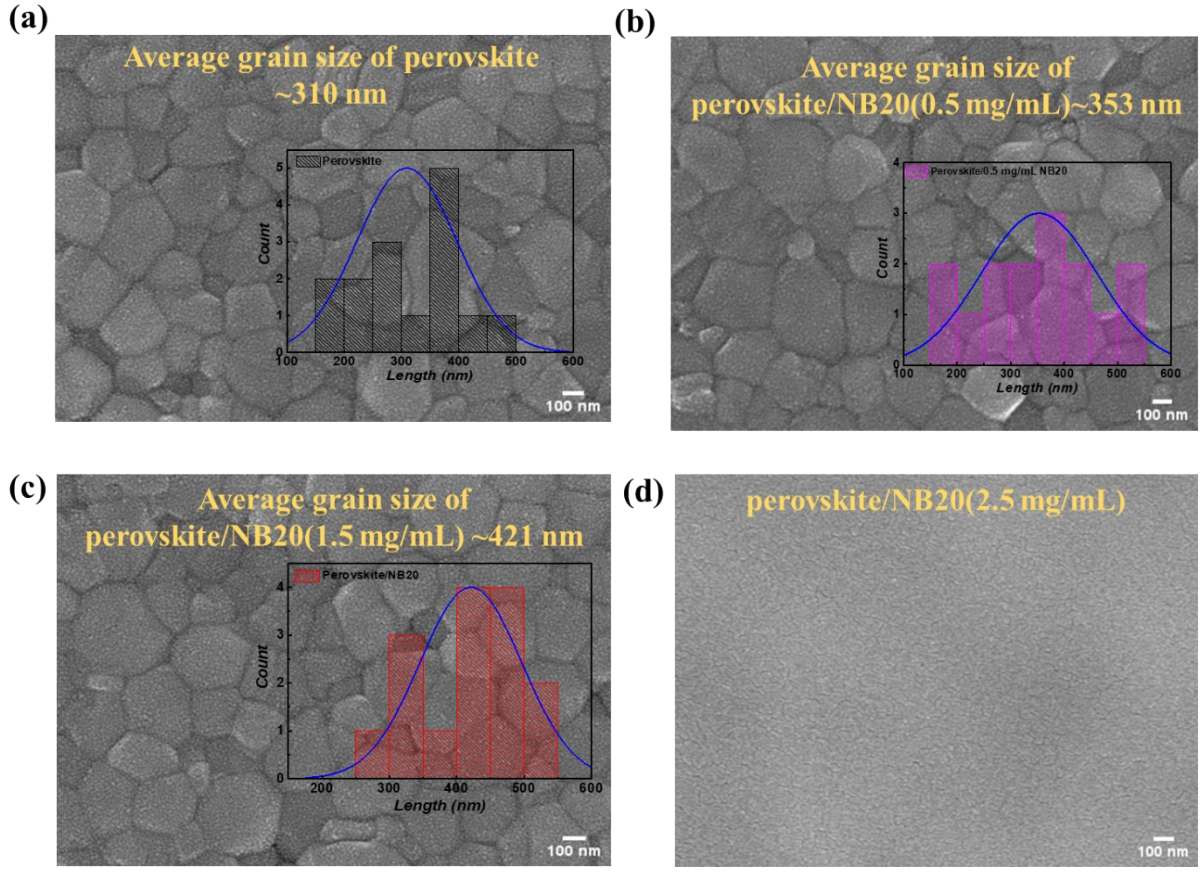

Figure S4. SEM images of perovskite films with NB20 at different concentrations: (a) 0 mg/mL, (b) 0.5 mg/mL, (c) 1.5 mg/mL and (d) 2.5 mg/mL.

4. Ultraviolet-Visible Spectroscopy:

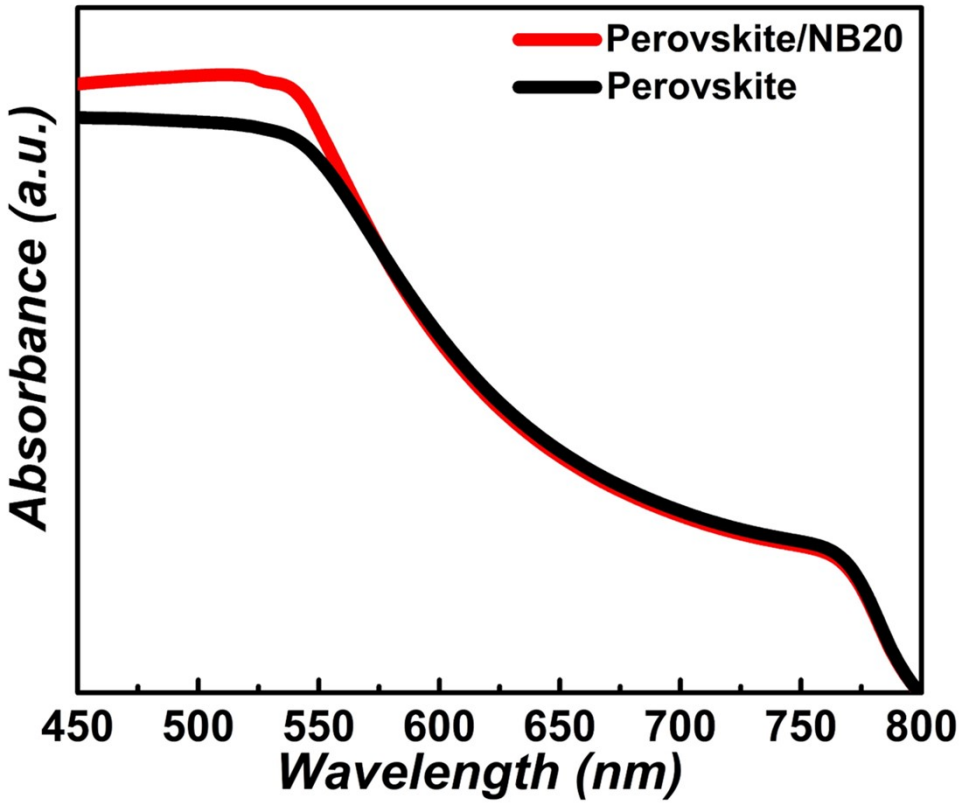

Figure S5. Absorbance spectra of UV-Vis revealing the optical characteristics of with and without NB20 film.

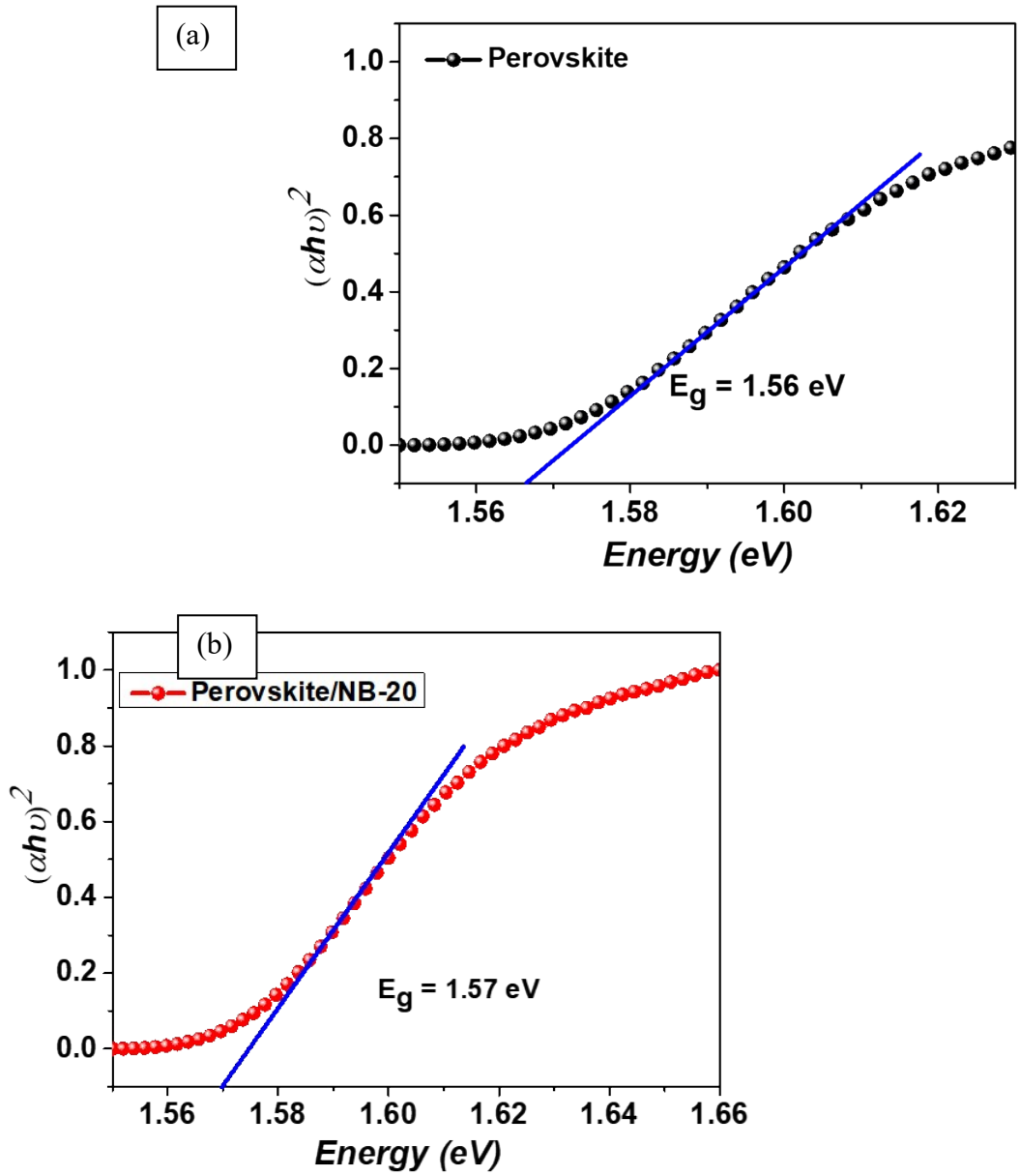

Figure S6. Optical band gap estimation using Tauc plot for (a) Perovskite and (b) NB20-treated Perovskite.

5. Time-resolved photoluminescence (TRPL) Spectra:

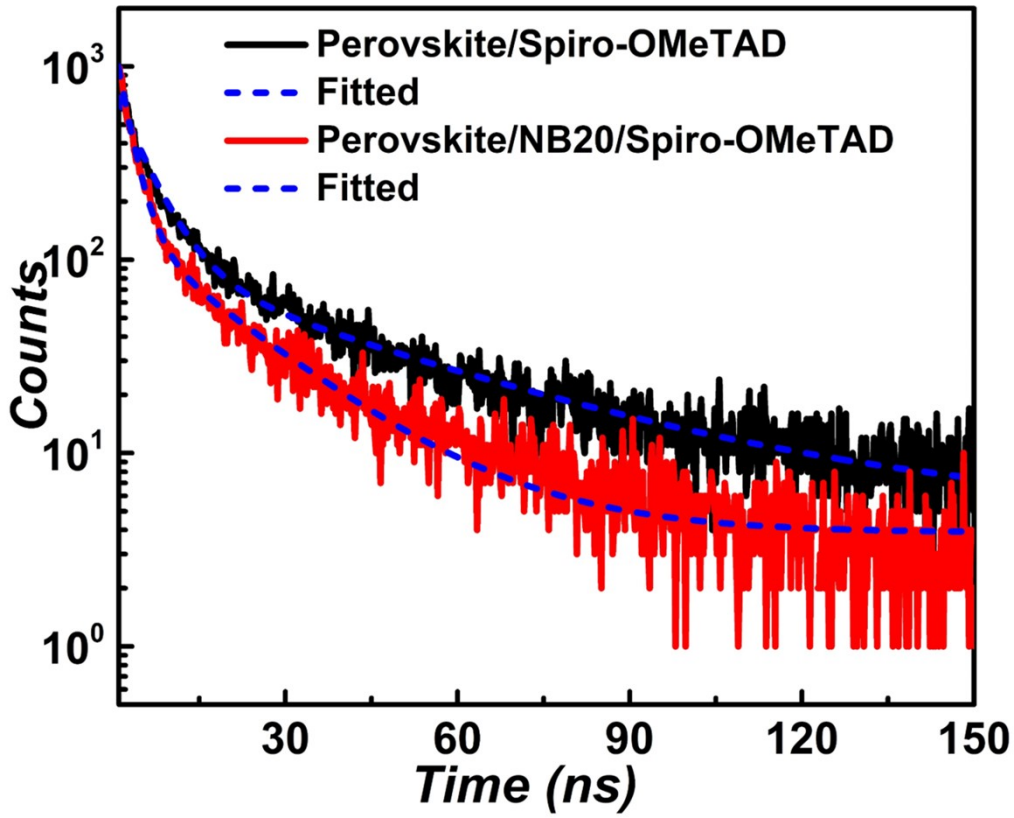

Figure S7. TRPL of analysis of base and NB20-passivated perovskite with Spiro-OMeTAD.

Table S1. Carrier lifetime summary derived from TRPL spectra fitting (**Figure S8**).

Samples	t_1 [ns]	A_1	t_2 [ns]	A_2	τ_{avg} [ns]
Perovskite/Spiro-OMeTAD	41.60	91.82	5.36	696.00	23.68
Perovskite/NB20/SpiroOMeTAD	18.49	144.71	2.39	1246.67	10.00

6. Current Density-Voltage (*J-V*) Characteristics

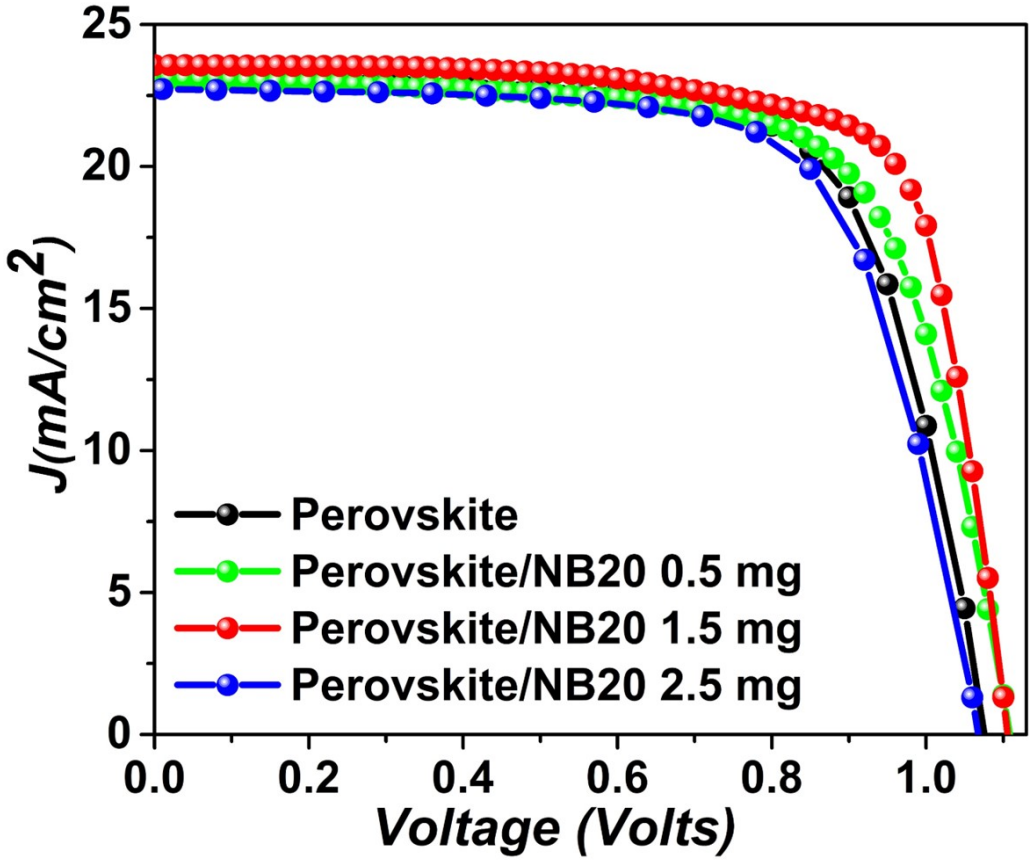

Figure S8. *J-V* Characteristic curves for various concentrations of the passivation Layer.

Table S2. Summarized of 15 devices average and champion (in bracket) photovoltaic parameters for varying **NB20** concentrations.

NB20 concentration [mg/ml]	Jsc [mA cm^{-2}] (Best)	Voc [V] (Best)	FF (Best)	PCE [%] (Best)
0	22.64 ± 0.25 (23.20)	1.08 ± 0.01 (1.08)	0.69 ± 0.01 (0.70)	16.96 ± 0.23 (17.48)
0.5	22.74 ± 0.32 (23.13)	1.10 ± 0.02 (1.11)	0.69 ± 0.01 (0.70)	17.28 ± 0.43 (17.85)
1.5	23.10 ± 0.37 (23.59)	1.11 ± 0.01 (1.12)	0.71 ± 0.01 (0.72)	18.18 ± 0.40 (19.02)
2.5	22.33 ± 0.42 (23.00)	1.06 ± 0.01 (1.07)	0.68 ± 0.01 (0.70)	16.05 ± 0.44 (16.93)

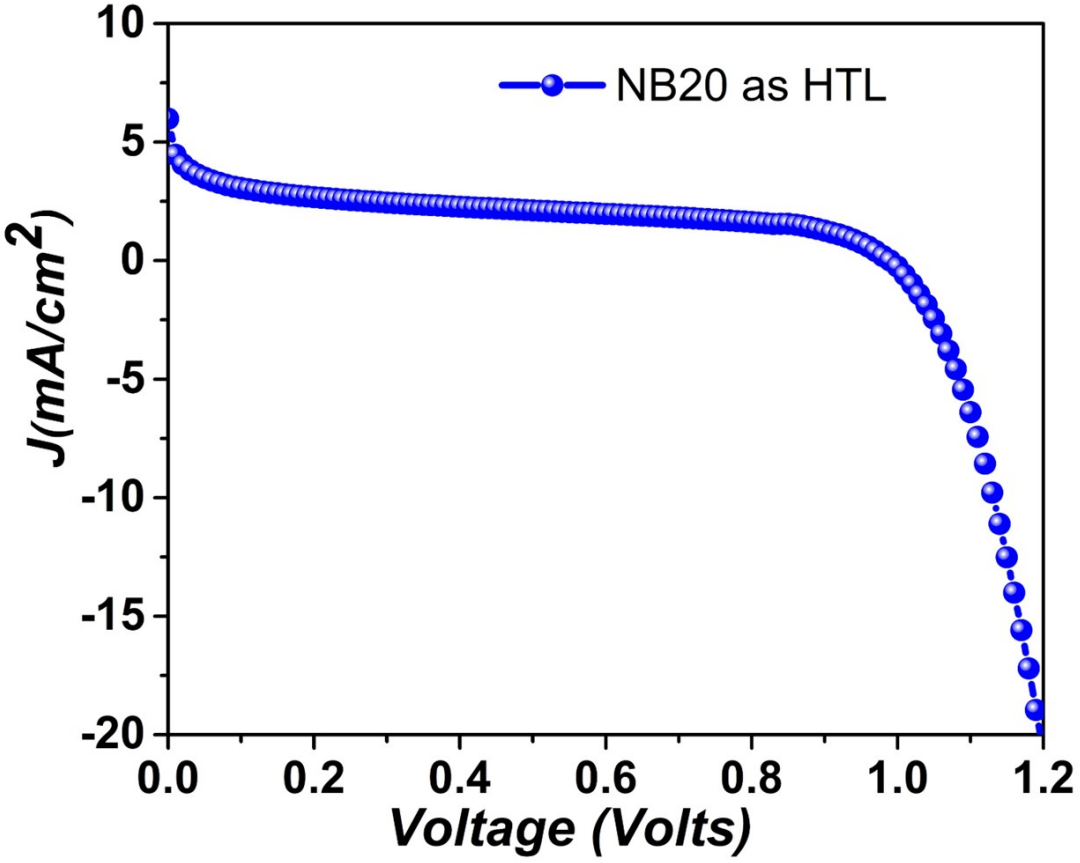

Figure S9. *J-V* Characteristic curves of PSCs using **NB20** as standalone HTL under AM1.5G illumination.

Table S3. Summary of the average photovoltaic parameters of four perovskite solar cell devices fabricated using **NB20** as the standalone HTL.

HTL NB20	J_{sc} (mA cm^{-2})	V_{oc} (V)	FF	PCE (%)
Device 1 (Best)	5.99	1.00	0.25	1.47
Device 2	5.39	0.99	0.25	1.35
Device 3	3.44	1.00	0.22	0.75
Device 4	4.56	0.65	0.27	0.81
Average	4.84 ± 1.10	0.91 ± 0.17	0.25 ± 0.02	1.10 ± 0.36

Fabrication Procedure for NB20-Based Hole Transport Layer

Cleaning, ETL deposition, and perovskite layer deposition were performed following the procedures described earlier in the manuscript. The **NB20** hole transport layer (HTL) solution was prepared by dissolving 90 mg of **NB20** in 1 mL of chlorobenzene. The resulting solution was spin-coated onto the perovskite layer at 3000 rpm for 30 s. Following HTL deposition, gold (Au) electrodes were thermally evaporated under a 10^{-6} bar vacuum, yielding devices with an active area of 9.9 mm^2.

7. Histogram Analysis

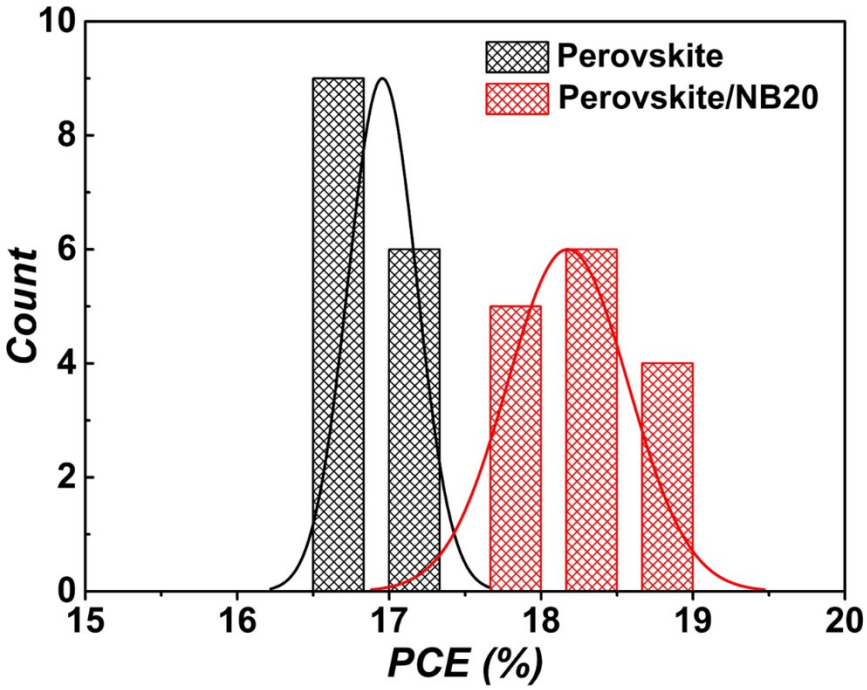

Figure S10. Histogram of PCE distribution from for base and NB20 modified devices.

8. Hysteresis Index Evaluation.

Table S4. Hysteresis Index calculation from *J-V* curves of with and without NB20 devices.

Device	J_{SC} [mA cm^{-2}]	V_{OC} [V]	Fill Factor	PCE [%]	HI
Perovskite Forward	22.58	1.08	0.69	16.75	
Perovskite Reverse	23.20	1.08	0.70	17.48	0.042
NB20 0.5 mg Forward	22.71	1.11	0.69	17.30	
NB20 0.5 mg Reverse	23.13	1.11	0.70	17.85	0.031
NB20 1.5 mg Forward	22.83	1.12	0.73	18.65	
NB20 1.5 mg Reverse	23.59	1.12	0.72	18.99	0.018
NB20 2.5 mg Forward	22.70	1.04	0.68	16.08	
NB20 2.5 mg Reverse	22.73	1.07	0.70	16.93	0.050

9. Electrochemical Impedance Spectroscopy (EIS):

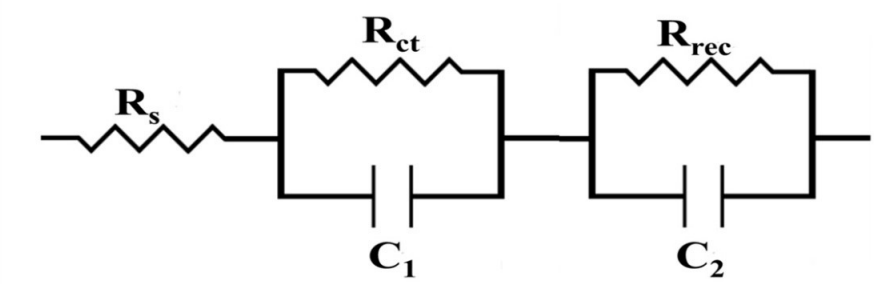

Figure S11. Equivalent circuit model for Nyquist plot in EIS analysis.

Table S5. Spectral parameters from EIS analysis for with and without **NB20** interlayer PSCs impedance.

Devices	Rs [Ω]	R_{ct} [Ω]	R_{rec} [Ω]	C_1 [F]	C_2 [F]	τ_{rec} [sec]
Perovskite	143.1	39 947	142321	5.25×10^{-9}	104.66×10^{-9}	7.48×10^{-4}
Perovskite/NB20	141.1	35 225	183727	5.59×10^{-9}	75.75×10^{-9}	10.3×10^{-4}

10. Fabrication of SCLC Devices for Mobility and Trap Density Analysis

To examine the trap density and charge carrier mobility in perovskite-based devices with and without an interlayer, two different hole-only configurations were fabricated and analysed using the space-charge-limited current (SCLC) technique. The first device, serving as the reference, had the structure ITO/PTAA/Perovskite/Au, while the second device incorporated a passivation layer, with the configuration

ITO/PTAA/Perovskite/NB20/Au [1]. The fabrication began with the preparation of pre-patterned indium tin oxide (ITO) substrates (Xinyan Technologies, Taiwan, 15 Ω/cm²). These substrates underwent a thorough cleaning procedure, involving ultrasonic treatment in a 5% Hellmanex III soap solution (Sigma-Aldrich) mixed with deionized water, followed by sequential rinsing in deionized water, acetone, and isopropyl alcohol (IPA) for 30 minutes each. After drying with nitrogen gas, the substrates were subjected to UV-ozone treatment (Bio-BEE Tech, India) at 70 C for 20 minutes to remove residual contaminants. To fabricate the hole-only devices, a 2 mg/ml PTAA solution in chloroform was spin-coated onto the pre-cleaned ITO substrates at 4000 rpm for 30 seconds. This was followed by annealing at 100 C for 10 minutes. The perovskite active layer was deposited via spin-coating, as detailed in the main manuscript. For the top electrode, an 80 nm thick gold (Au) layer was deposited using a thermal evaporator, ensuring uniform coverage and stable contact [2]. To complete the SCLC device, an 80 nm Gold (Au) layer was thermally evaporated (Hind High Vacuum, India) under a vacuum pressure of 1 $\times 10^{-6}$ mbar. The active area of the fabricated devices, determined by the overlapping region of the ITO and the top electrode, measured 0.066 cm². The thickness of each layer was confirmed using a Dektak surface profiler. Once fabrication was completed, the devices were immediately subjected to current-voltage (*J-V*) characterization using a Keithley 2400 dual-channel source meter[3].

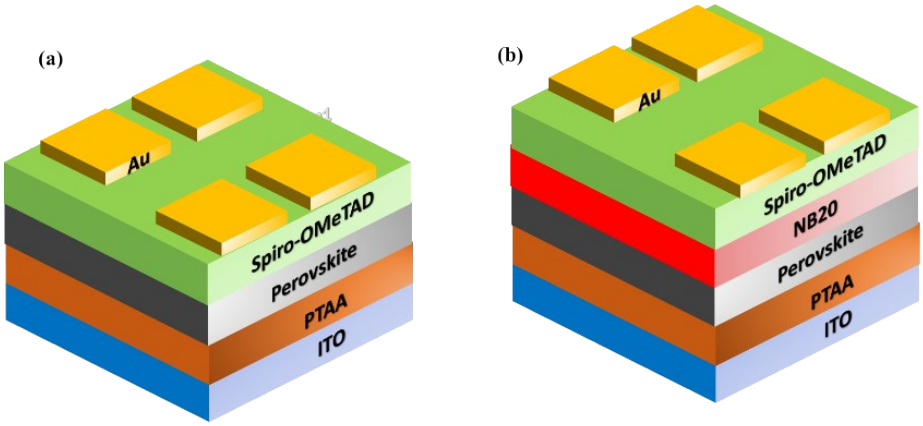

Figure S12. Illustration of Hole-Only devices (a) Bare perovskite (b)NB20 passivated perovskite.

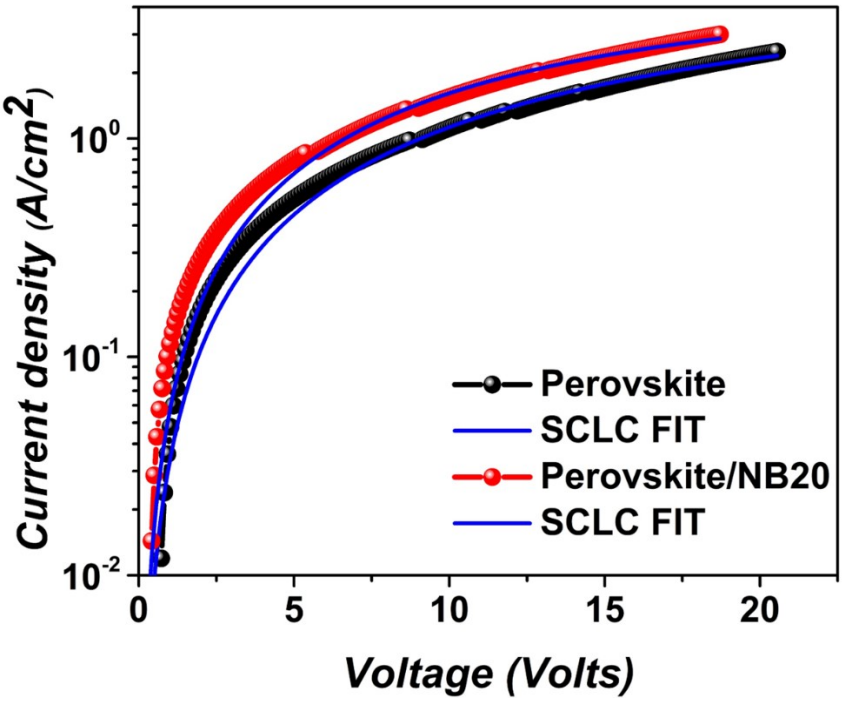

Figure S13. SCLC-based mobility calculation for devices shown in **Figure S12**. *J-V* characteristics were analysed using the Mott-Gurney law to compare charge transport properties.

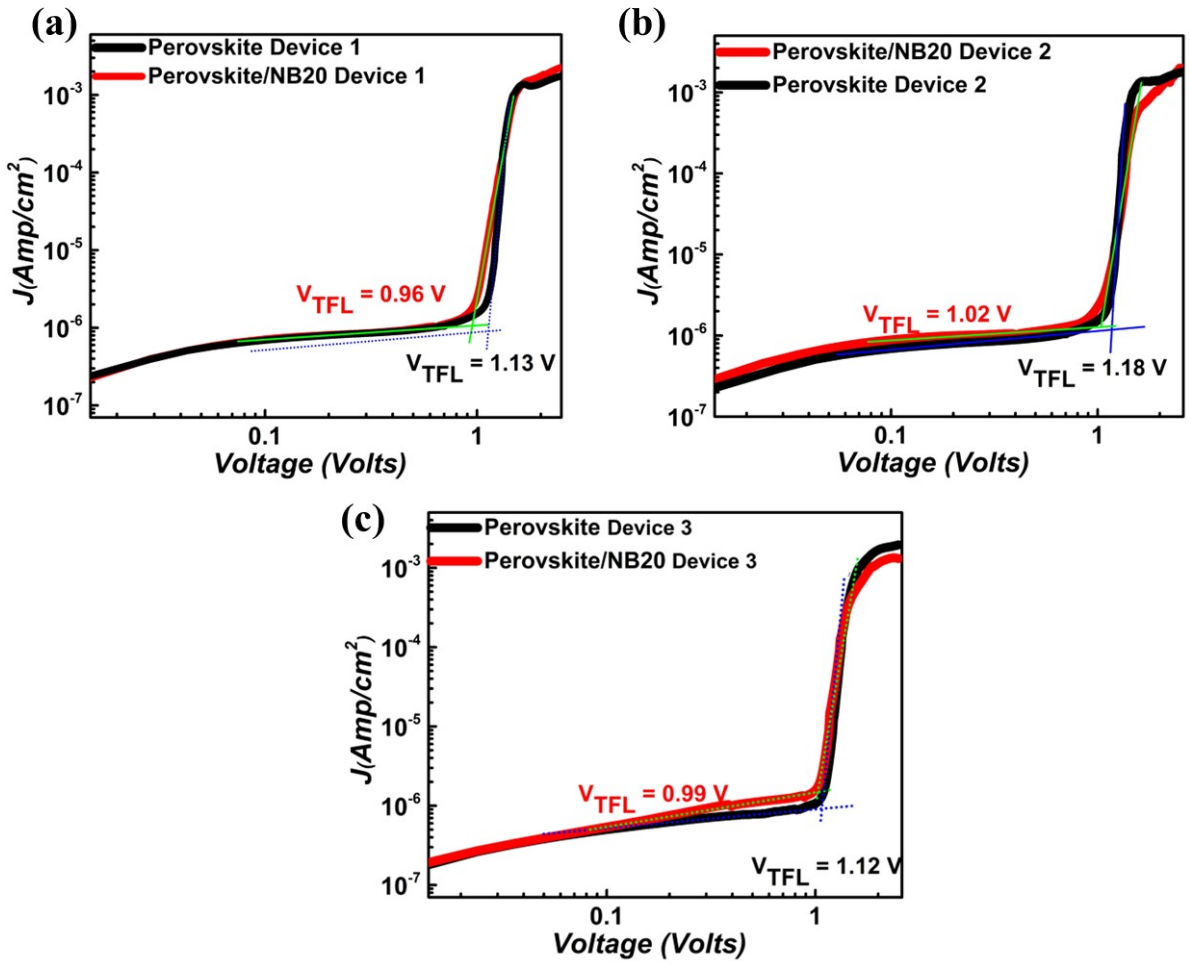

Figure S14. *J-V* characteristics of hole-only devices used to evaluate the trap density in the active material for (a) Device 1, (b) Device 2, and (c) Device 3. The trap-filled limit voltage extracted from each curve is used to calculate the corresponding trap density.

Table S6. Summary of the extracted trap density values for the three devices with and without the NB20 interlayer, along with the percentage reduction in trap density.

Device	**Perovskite** η_{trap} **(x 10^{16} cm^{-3})**	**Perovskite/NB20** η_{trap} **(x 10^{16} cm^{-3})**	Δ (%)
1	2.19	1.86	15.07
2	2.30	1.98	13.00
3	2.18	1.93	11.47
Average	2.22 ± 0.07 **(3.15%)**	1.92 ± 0.06 **(3.13%)**	13.18 ± 1.81 **(13.73%)**

11. References

1 K. Sivula, *ACS Energy Lett.*, 2022, **7**, 2102–2104.

2 M. Warish, G. Jamwal, Z. Aftab, N. Bhatt and A. Niazi, *ACS Appl. Electron. Mater.*, 2023, **5**, 5432–5445.

3 V. M. Le Corre, E. A. Duijnstee, O. El Tambouli, J. M. Ball, H. J. Snaith, J. Lim and L. J. A. Koster, *ACS Energy Lett.*, 2021, **6**, 1087–1094.